

Chapter 3 Experimental Setup

3.1 Introduction

The plasma focus system includes the charger, capacitor, focus chamber and the vacuum system. The design of the focus chamber is made to suit the needs of various diagnostics. The diagnostic ports and the connecting parts to the focus chamber can be rearranged based on the experiments. The diagnostic tools employed are Rogowski coil, resistive voltage divider, X-ray diode (XRD), EUV detector and biased ion collectors.

3.2 Plasma Focus System Design

The plasma focus discharge is driven by two Maxwell capacitors with each rated at 60 kV, 1.85 μF and connected in parallel to obtain a total capacitance of 3.7 μF . In the current project, the capacitor bank will be charged to 18 kV and this gives a total of 600 joules of stored energy. The capacitor bank is connected to the plasma focus tube via a spark gap. The focus chamber that houses the electrodes is evacuated by a turbo-molecular pump back-up by a rotary pump. The operating gas is introduced into the chamber through a flow rate controller.

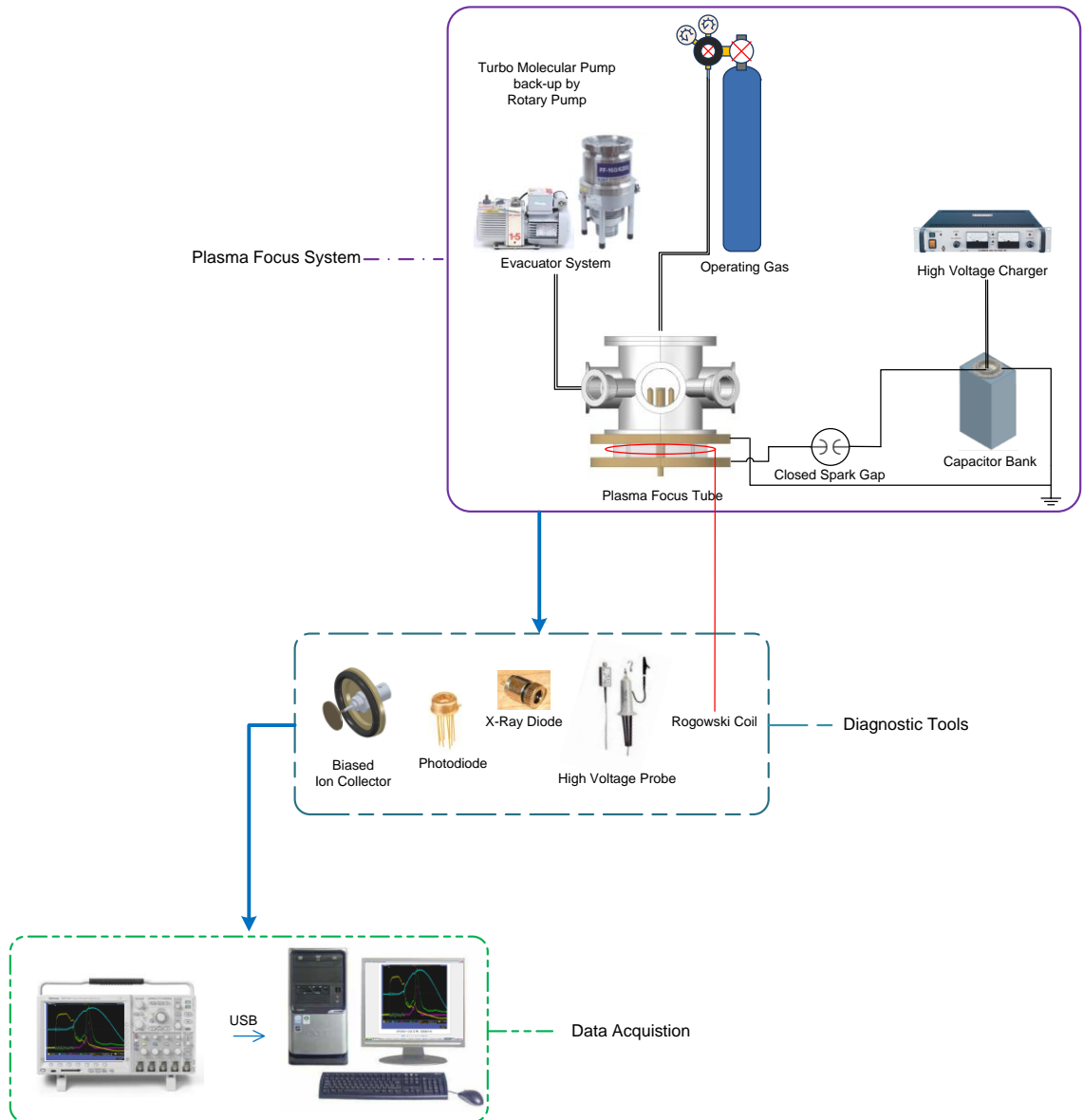


Figure 3.1 Block diagram of the entire plasma focus experimental setup.

Figure 3.1 illustrate the block diagram of the 600 joules Mather type small plasma focus system. This plasma focus system consists of the following sub-systems:

- i. The plasma focus device
 1. Plasma focus tube
 2. Capacitor bank
 3. High voltage charger with single pulse triggering system
 4. Spark gap
 5. Vacuum system consisting of turbo molecular pump back-up by rotary pump
- ii. Diagnostic tools
 1. Rogowski Coil
 2. Resistive voltage divider
 3. X-ray Diode (XRD)
 4. EUV detector
 5. Ion beam detectors
- iii. Data Acquisition
 1. Digital oscilloscope
 2. Interfacing System
 3. Computer

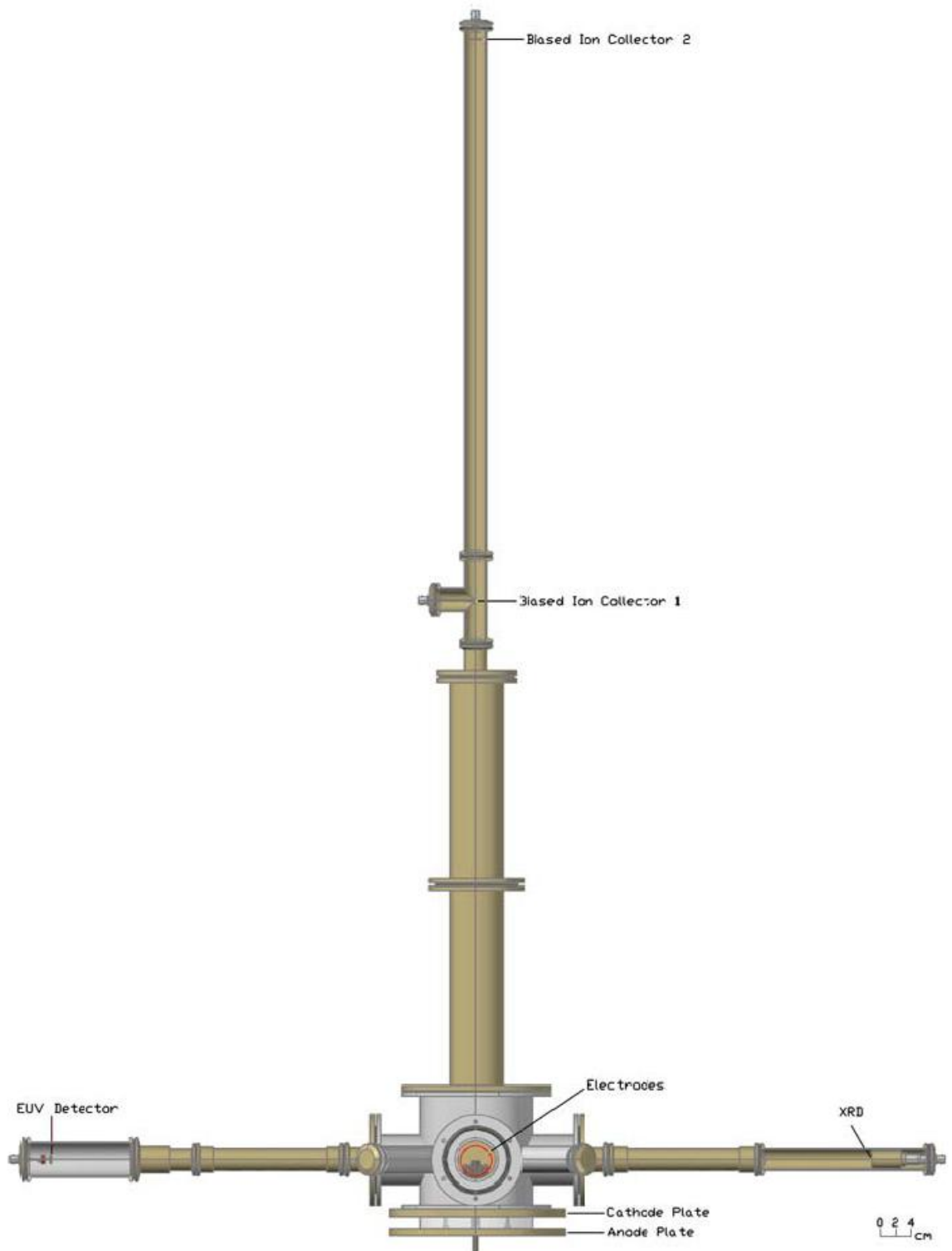


Figure 3.2 The 3D drawing of the small plasma focus system complete with the three diagnostic ports.

Figure 3.2 shows the 3D drawing of the plasma focus system. The discharge current and the discharge voltage are measured by using a Rogowski coil and a resistive voltage divider respectively. X-ray diode (XRD) is used as broadband X-ray detector. It is mounted at a side-on observation port 550 mm from the anode tip, while the EUV detector is mounted on another side-on observation port, at a distance of 550 mm from the anode tip. The ion beam is measured by using two biased ion collectors placed at 70 cm and 140 cm from the anode in the axial direction.

Table 3.1 shows the system parameters for this 600 joules small plasma focus. The system inductance and resistance are the short circuit inductance and resistance of the system.

Table 3.1 System parameters of the 600 joules small plasma focus.

Bank Parameters		Tube Parameters		Operating Parameters	
Capacitance, C_o	3.7 μ F	Anode radius, a	4.75 mm	Voltage, V_o	18 kV
Inductance, L	128.3 ± 1.4 nH	Cathode radius, b	23.75 mm	Pressure, P	$\sim 10^{-2}$ mbar
Resistance, r	23.5 ± 0.3 m Ω	Anode length, z	60.00 mm	Operating Gas	Argon

3.3 Diagnostics Techniques

In the current project, several diagnostic techniques are employed to measure the ultra-soft X-radiation, EUV and the ion beams as well as the electrical parameters of the plasma focus discharge. Owing to the limited number of diagnostic ports available, not all the measurements are carried out simultaneously.

3.3.1 Discharge Current Measurement

Rogowski coil is used to measure the pulsed discharge current. It is a multi-turn torus-shaped solenoid and made by inserting a surface insulated copper wire into a thick plastic hose. It is placed behind the backwall of the focus tube encircling the inner electrode. The schematic drawing of the Rogowski coil is shown in Figure 3.3.

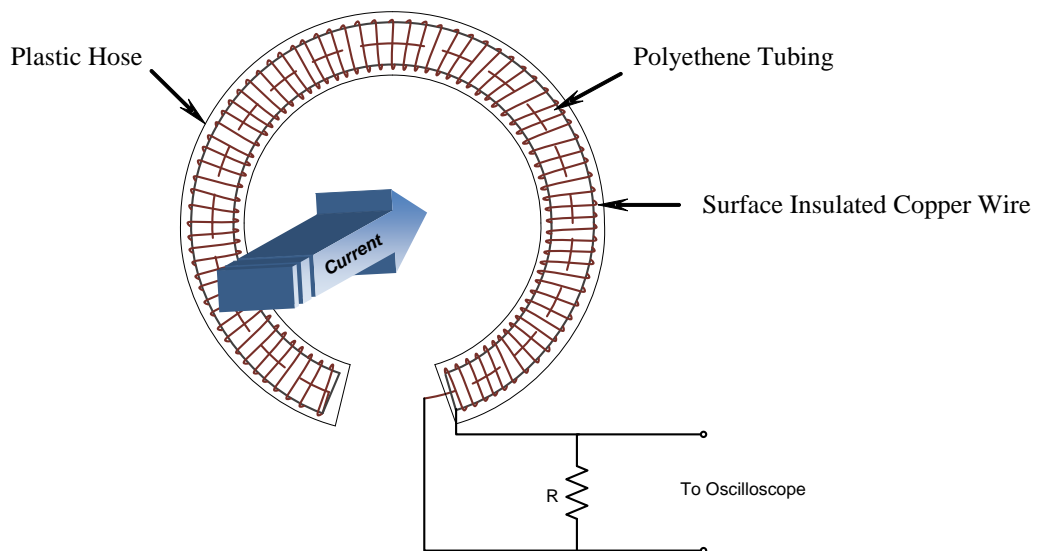


Figure 3.3 Schematic diagram of the Rogowski coil.

According to Faraday's law, an electromotive force, $-d\Phi/dt$ will be induced by the time-varying magnetic field, where Φ is the magnetic flux threading the coil. This force will cause current flow in the solenoid. Thus by measuring the magnetic field

induced by the time-varying electric current flowing through the plasma, the current can be measured.

From Ampere's law, the induced magnetic field or the magnetic flux that threads the coil is proportional to the current $I(t)$. The induced voltage across the terminals of the coil is the sum of the electromotive force of each minor coil. The induced voltage is proportional to the rate of change of the current, dI/dt , not the current itself. In order to obtain $I(t)$, the coil output voltage must be integrated. This can be done by operating the Rogowski coil in a current transformer mode, i.e. by shorting its terminals with a small resistance, $R \sim 0.1 \Omega$ as shown in Figure 3.4.

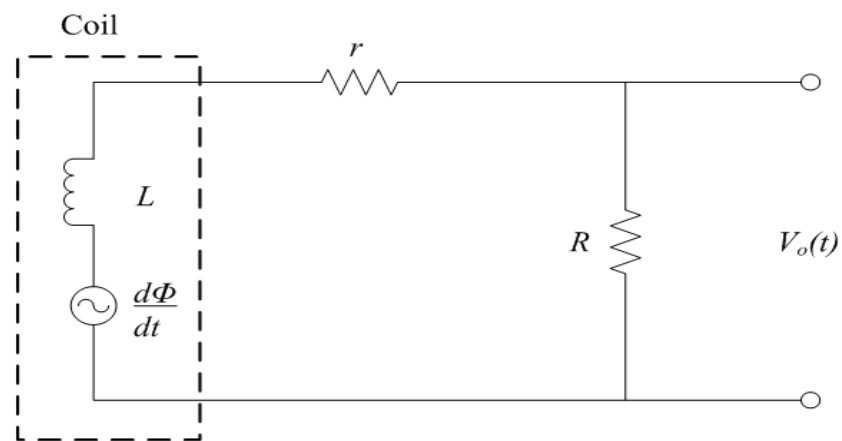


Figure 3.4 Rogowski coil operated in the current transformer mode.

The circuit equation is given by

$$V(t) = L \frac{dI}{dt} + i(r + R) \quad (3.1)$$

where r is the coil resistance, which is usually negligible, and L is the coil inductance. If R is chosen to be small enough such that $L\omega \gg (r + R)$, high frequency current can be measured and the Equation (3.1) can be simplified to Equation (3.2).

$$\begin{aligned} V(t) &= L \frac{dI}{dt} \\ &= \frac{d\phi}{dt} \end{aligned} \quad (3.2)$$

and

$$\begin{aligned} i(t) &= \frac{1}{L} \int_0^t V(t) dt \\ &= \frac{\phi}{L} \end{aligned} \quad (3.3)$$

where $\phi = \frac{\mu_o N A I(t)}{2\pi a R}$ and $L = \frac{\mu_o N^2 A}{2\pi a R}$.

Equation (3.3) can be written as:

$$\begin{aligned} i(t) &= \frac{\frac{\mu_o N A I(t)}{2\pi a R}}{\frac{\mu_o N^2 A}{2\pi a R}} \\ &= \frac{I(t)}{N} \end{aligned} \quad (3.4)$$

According to Ohm's Law, $I = V/R$, therefore

$$\begin{aligned} V_o(t) &= iR \\ &= \frac{R}{N} I(t) \end{aligned} \quad (3.5)$$

where V_o is the output voltage across R . Thus, the output voltage will give a direct measurement of the main current with the expression below.

$$\begin{aligned} V &= \frac{RI}{N} \\ &= KI \end{aligned} \quad (3.6)$$

where R is the small external resistance, N is the number of the turns of the Rogowski coil, I is the discharge current flowing in the plasma focus system and K is the calibration factor of the coil.

3.3.1.1 Calibration of the Rogowski Coil

The Rogowski coil is calibrated to allow the measurement of the absolute value of the discharge current. The coil is calibrated based on the equation mentioned above, as it is not practical to measure the geometry of the coil which include the number of solenoid turn, N radius of the torus, A and radius of the minor cross section, a and the small resistance used to short the coil accurately. In this work, the Rogowski coil calibration is done by using the in-situ method, that the short circuit current is measured with the coil in place of the actual experiment.

The discharge current waveform is analyzed. The circuit equation is given as

$$L\left(\frac{dI}{dt}\right) + IR + \frac{\int Idt}{C} = V_o \quad (3.7)$$

For a lightly damped discharge, $R < 2\sqrt{L/C}$, the solution of the Equation (3.7) is a form of damped sinusoid given by Equation (3.8).

$$I(t) = I_o e^{-\alpha t} \sin \omega t \quad (3.8)$$

where

$$I_o = V_o \sqrt{\frac{C}{L}}$$

$$\alpha = \frac{R}{2L} \quad (3.9)$$

$$\omega = \frac{1}{\sqrt{LC}}$$

From the current waveform, the periodic time, T and the reversal ratio, f_r can be measured, thus

$$\alpha = -\frac{\ln(f_r)}{T} \quad (3.10)$$

where

$$f_r = \frac{1}{n-1} \sum_1^{n-1} \frac{V_{i+1}}{V_i} \quad (3.11)$$

At the first peak of the current where $t = T/4$,

$$I_1 = I_o e^{-\alpha T/4}$$

$$= \frac{\pi C_o V_o (1 + f_r)}{T} \quad (3.12)$$

Hence the calibration factor of the coil can be obtained as Equation (3.13).

$$K = \frac{I_1}{V_1} = \frac{\pi C_o V_o (1 + f_r)}{TV_1} \quad (3.13)$$

The lightly damped sinusoidal discharge current waveform at high pressure, in this case 5.0 mbar is illustrated in Figure 3.5. The calibration factor of the coil, K by using the in-situ method is 7.6 ± 0.2 kA/V.

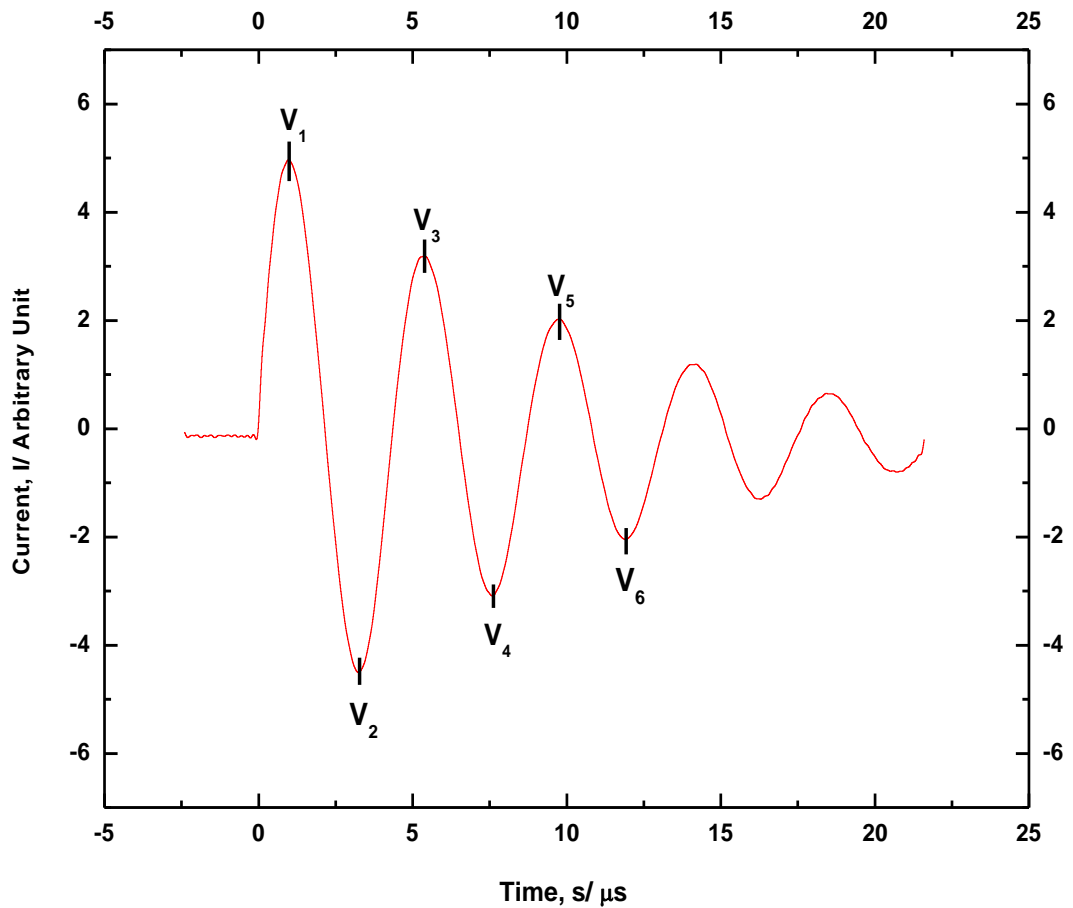


Figure 3.5 Lightly damped sinusoidal waveform for calibration factor of a Rogowski coil.

3.3.2 Discharge Voltage Measurement

Resistive voltage divider is used to measure the transient voltage across the plasma. This probe consists of a series of ten low inductance resistors, $510\ \Omega$ connected in series and shunted by a $51\ \Omega$ resistor at one end of the chain. The resistor chain is enclosed in a 20 mm diameter copper tube. The insulation between the copper tube and the resistor chain is provided by a PVC hose. The voltage probe is mounted across the anode and the cathode of the plasma focus tube via the anode plate and the cathode plate. Figure 3.6 shows the schematic drawing of the resistive voltage divider.

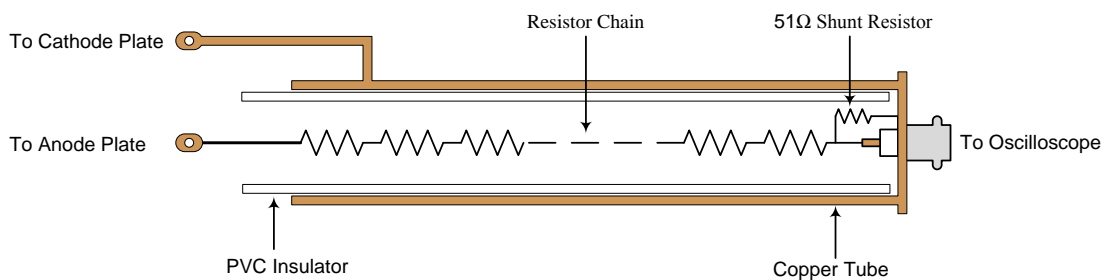


Figure 3.6 Schematic diagram of the resistive voltage divider.

The voltage signal is terminated with a ten times attenuator with a matching load of $51\ \Omega$. The probe is calibrated against a Tektronix high voltage probe. The attenuation factor is 2200. The rise time of the probe is found to be less than 2.6 ns.

3.3.3 Ultra-Soft (UV-EUV) Radiation Measurement

X-ray Diode (XRD) is generally used as broadband X-ray detector. It has a spectral sensitivity range from UV to soft X-ray, which is 6\AA to 600\AA . The principle operation of XRD is based on the photoelectric effect. A photocurrent of ejected secondary electrons that are generated by absorption of photons incident on the active photocathode surface. The registered photocurrent is proportional to the intensity of the incident radiation. Figure 3.7 shows the operation of the XRD.

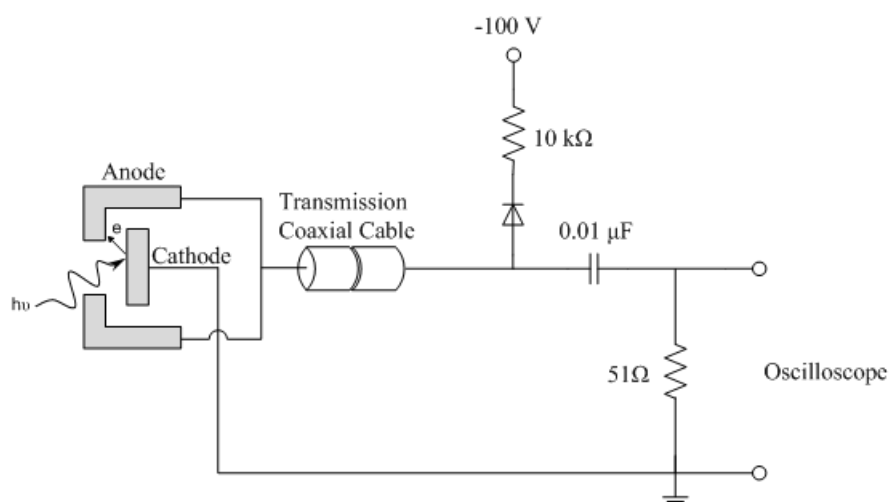


Figure 3.7 The operation and the schematic diagram of the XRD.

In this work, an aluminum active photocathode surface with a brass wire mesh anode mounted above the cathode is employed. The diode is mounted at the side observation port of the vacuum chamber at a distance of 550 mm from the plasma. The mesh provides little attenuation to the incident flux. The XRD is negatively biased at a voltage of 100V. This is sufficient to collect all electrons emitted by the cathode in response to the incident photons. The entire XRD is placed inside the copper gasket that acts as faraday shield to minimize stray charges and noises.

3.3.4 EUV Measurement

EUV in the range of 11 nm -18 nm is investigated by using a fast filtered photodiode, SXUV5A with integrated thin film filters of 100 nm Si/ 200 nm Zr. Typical visible light transmission of this filtered diode is less than 10^{-4} .

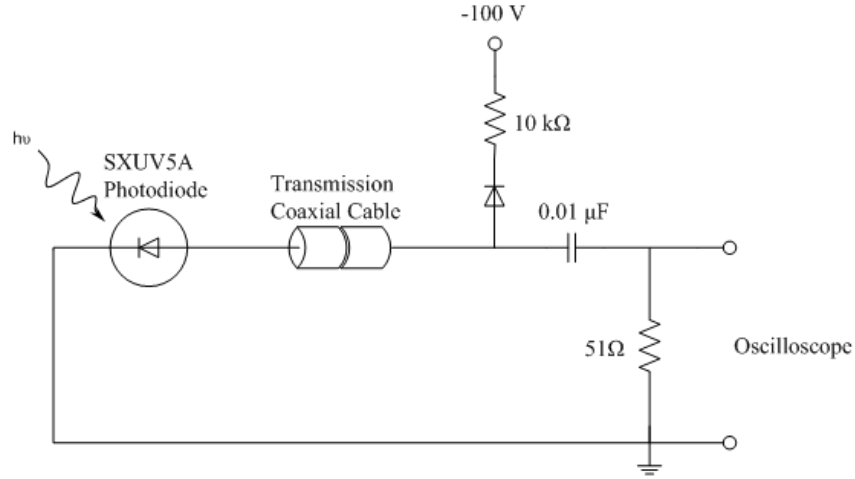


Figure 3.8 The schematic diagram of the EUV detector.

Photodiode SXUV5A is placed at 550 mm from the plasma at the side observation port. A biasing circuit is used to reverse bias the SXUV5A up to 100V. Figure 3.8 shows the schematic diagram of the EUV photodiode. The total charge of the electrons, Q generated in the photodiode per pulse can be calculated by integrating the voltage signal and expressed as Equation (3.14).

$$Q = \frac{1}{R} \int V dt \quad \text{Coulombs} \quad (3.14)$$

The sensitivity of SXUV5A at the wavelength of 13.5 nm is 0.194 A/W and the quantum efficiency of this diode is about 9.23 C/J. The specifications of the fast filtered

photodiode SXUV5A is shown in Table 3.2. The responsivity and the filtered quantum efficiency of this photodiode are shown in Figure 3.9 and Figure 3.10, respectively.

Table 3.2 Specification data of the EUV detector, IRD-SXUV5A with integrated thin film filters of 100 nm Si/ 200 nm Zr.

Specification	Data
Sensitivity/ Responsivity (A/W)	0.194 at 13.5 nm
Filtered Quantum Efficiency (C/J)	9.23 at 13.5 nm
Sensitive area (mm ²)	5
Size (mm)	2.5 Ø
Shunt resistance (MΩ)	200
Capacitance at 0V (nF)	1
Rise time (n sec)	500

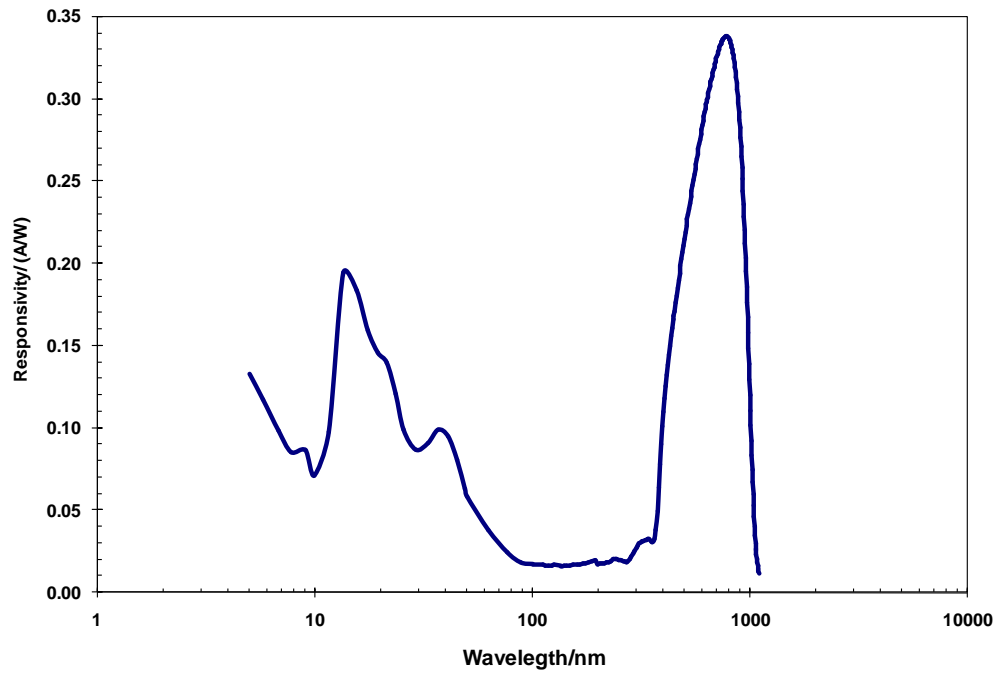


Figure 3.9 Responsivity for EUV detector, SXUV5A.

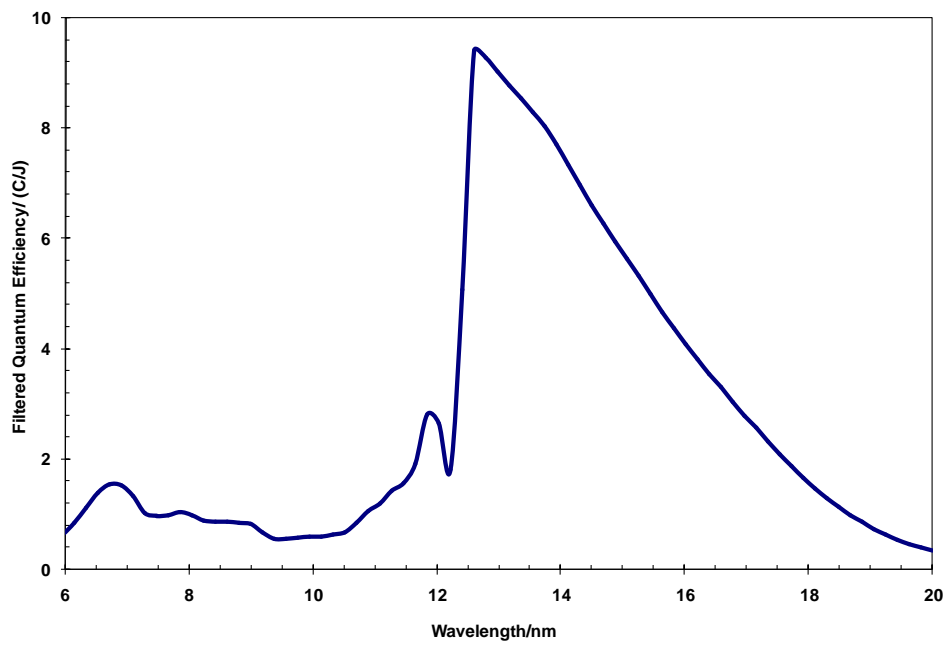


Figure 3.10 Filtered quantum efficiency for EUV detector, SXUV5A.

In order to confirm that this detector does not register photons of lower energy in UV to visible, a quartz plate is used to filter the EUV emission. In discharges where emissions are measured, no signal is detected by the photodiode. This indicates the fast filtered photodiode, SXUV5A is not detecting the UV and visible light emission from the plasma source.

3.3.5 Ion Beam Measurement

The ion beam emitted by plasma focus system is measured by a biased ion collector. It is connected to the biasing circuit via a coaxial cable. The collector pickup ions from the passing ion beam without disturbing the ion beam energy distribution, ion velocity and other parameters. The schematic diagram of a biased ion collector is shown in Figure 3.11.

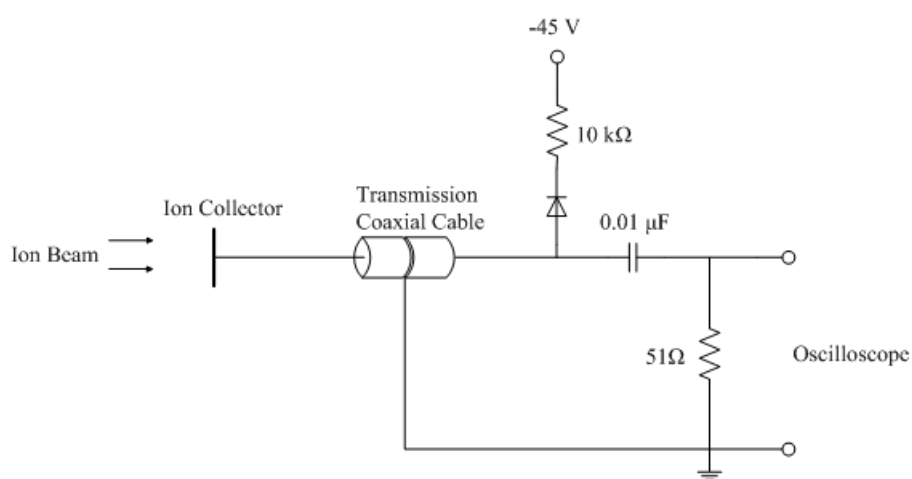


Figure 3.11 The schematic diagram of a biased ion collector.

In the current set-up, two simple biased ion collectors made of copper plates are employed. The first and the second collectors have different detection areas of 30.24 mm^2 and 927.6 mm^2 , respectively. They are placed along the axis of the electrodes at different positions inside the collimator and they are arranged in a way such that the ion beam will not be blocked by the first collector. Figure 3.12 shows the arrangement of these two biased ion collectors. Time-of-Flight (TOF) analysis can be employed to determine the ion beam energy.

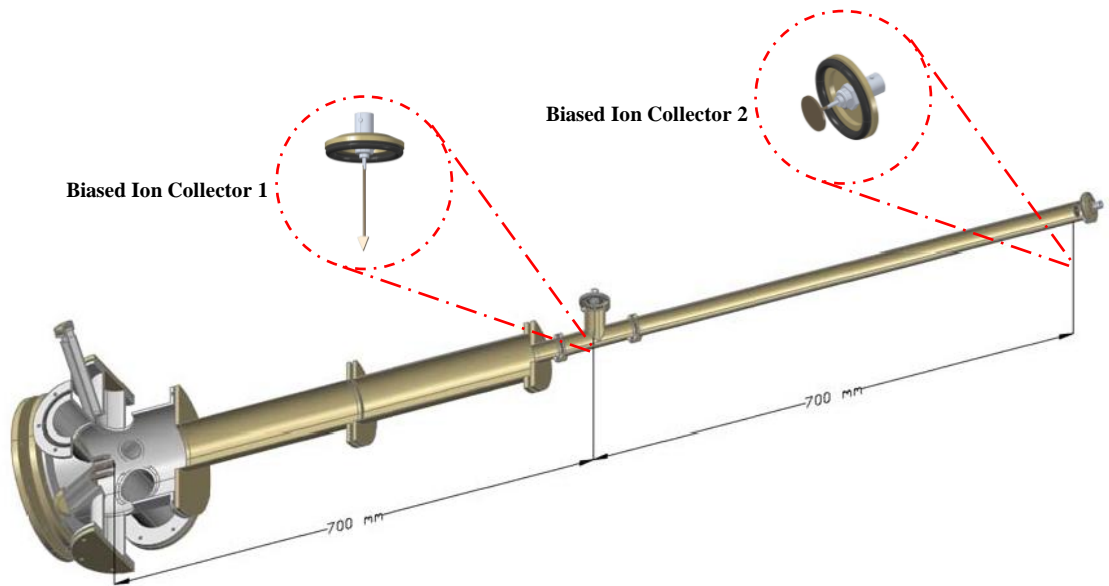


Figure 3.12 The arrangement of the two biased ion collectors.